EMBO reports

scientific report

Structural rearrangements in tubulin following microtubule formation

Angelika Krebs[+], *Kenneth N. Goldie & Andreas Hoenger*
European Molecular Biology Laboratory, Heidelberg, Germany

Microtubules are essential cytoskeletal structures that mediate several dynamic processes in a cell. To shed light on the structural processes relating to microtubule formation and dynamic instability, we investigated microtubules composed of 15 protofilaments using cryo-electron microscopy, helical image reconstruction and computational modelling. Analysis of the configuration of the αβ-tubulin heterodimer shows distinct structural differences in both subunits, and illustrates that the tubulin subunits have different roles in the microtubule lattice. Our modelling data suggest that after GTP hydrolysis microtubules, adopt a conformational state somewhere between a straight protofilament conformation—as found in zinc-induced tubulin sheets—and an outward curved conformation—as found in tubulin–stathmin complexes. The tendency towards a curved conformation seems to be mediated mostly by β-tubulin, whereas α-tubulin resembles a state more related to the straight structure. Our data suggest a possible explanation of dynamic instability of microtubules, and for nucleotide-sensitive microtubule-binding properties of microtubule-associated proteins and molecular motors.

Keywords: microtubule; tubulin dimer; electron microscopy; straight tubulin conformation; curved tubulin conformation
EMBO reports (2005) **6**, 227–232. doi:10.1038/sj.embor.7400360

INTRODUCTION

Microtubules are essential components of the cytoskeleton, having important roles in cell motility and cell morphogenesis (Hyams & Lloyd, 1994; Amos, 2000; Downing, 2000). They are highly dynamic structures (Mitchison & Kirschner, 1984; Desai & Mitchison, 1997; Nogales, 2001; Howard & Hyman, 2003) and, *in vivo*, their stability is tightly regulated by microtubule-associated proteins (Hirokawa, 1994; Mandelkow & Mandelkow, 1995).

The basic structural unit of microtubules is the αβ-tubulin dimer. Tubulin dimers arrange head to tail to form protofilaments that associate laterally into a polar microtubule structure. Both α- and β-tubulin consist of around 450 amino acids, with a high similarity in sequence (40% sequence homology; Ludveňa, 1998). Both subunits bind GTP, but only in β-tubulin is GTP hydrolysed following polymerization, with a slight lag phase. This lagging hydrolysis forms a so-called GTP cap at the plus end of growing microtubules (reviewed by Nogales, 2001), preventing the tubes from falling apart. Hence, within the microtubule, the α-tubulin subunit contains GTP, whereas the β-tubulin subunit carries GDP. Because reconstituted kinetochores from *Saccharomyces cerevisiae* are able to distinguish between different structural states of a GDP- and a GTP-microtubule lattice (Severin *et al*, 1997), it is probable that GTP hydrolysis induces a recognizable structural change in the microtubule lattice.

Tubulin dimers not only form tubular structures, but also two-dimensional crystalline sheets with $p12_1$ symmetry (Downing & Jontes, 1992), where protofilaments are arranged in an antiparallel manner (Zn-sheets). Such crystalline arrangements yielded an electron density map of tubulin dimers to 3.7 Å resolution (Nogales *et al*, 1998), where both subunits seem structurally similar. The structural data from Zn-sheets were used to build a high-resolution model of the microtubule (Nogales *et al*, 1999), which was later refined using an 8 Å resolution map of a 13-protofilament microtubule (Li *et al*, 2002).

Despite the detailed model of microtubules, the molecular mechanism for dynamic instability is poorly understood. Recently it has become clear that microtubules are not just sturdy tracks, but participate on their own in the cellular transport and dynamic processes of a cell. Of great interest in this context is the X-ray crystal structure of tubulin complexed with colchicine and a stathmin-like domain (Ravelli *et al*, 2004), which demonstrated that structural changes within the tubulin core are probably the key features in such a process. Recently, we reported new structural results on three-dimensional (3D) reconstructions of helical microtubules (Krebs *et al*, 2004). We described significant differences in the conformation of the tubulin dimer in plain microtubules versus microtubules complexed with kinesin motors, and could show that these structural differences are the result of motor binding to the outside of β-tubulin. The binding of motor domains, it seems, has a strong stabilizing effect axially along the microtubule protofilaments.

In accordance with these results, this work aims to investigate the structural involvement of tubulin in the dynamic instability of microtubules. Krebs *et al* (2004) were the first to describe structural differences between α- and β-tubulin observed on an

European Molecular Biology Laboratory, Meyerhofstrasse 1, 69117 Heidelberg, Germany
[+]Corresponding author. Tel: +49 6221 387 8815; Fax: +49 6221 387 306;
E-mail: krebs@embl-heidelberg.de

Received 4 October 2004; revised 17 January 2005; accepted 28 January 2005; published online 25 February 2005

©2005 EUROPEAN MOLECULAR BIOLOGY ORGANIZATION

intermediate-resolution cryo-electron microscopy (cryo-EM) 3D-map. To further investigate the nature of these differences, we used the Zn-sheet dimer structure (Nogales *et al*, 1998) to obtain an initial best-possible fit into our 3D-map, under the assumption that tubulin dimers in Zn-sheets and microtubules are similar. We then refined the positions of α- and β- tubulin separately, using rigid-body refinement. The resulting 'microtubule-tubulin-dimer' model was then compared with the straight dimer conformation, which was used initially (Zn-sheets; Nogales *et al*, 1998), and with the curved conformation found in the tubulin–stathmin complex (Ravelli *et al*, 2004). Our data led to a model for the tubulin dimer in microtubules, which resembles an intermediate state between straight and curved. β-Tubulin seems to adopt a conformation related to the curved state, whereas α-tubulin more probably resembles a configuration related to the straight structure. The resulting curvature of the tubulin dimer in the microtubule lattice indicates the potential of the dimers to assume the outward-bent ram-horn-like configuration, as found following depolymerization. The microtubule lattice constraints, however, seem to act against this outward bending, and thereby force the dimer into an intermediate state.

RESULTS AND DISCUSSION

Electron density and modelling

Our structural work on microtubules is consistently carried out on helical 15-protofilament microtubules, thus avoiding the complications arising from seams (found in the naturally occurring, more common, 13-protofilament microtubules). At a seam, lateral contacts are between different tubulin subunits (between α- and β-tubulins), whereas all other lateral microtubule contacts are between similar subunits (α–α contacts and β–β contacts). From helical microtubules with 15 protofilaments, we calculated a density map to a resolution of 17 Å using an improved image processing protocol (described in detail by Krebs *et al*, 2004), which allowed us to distinguish between α- and β-tubulin. In the electron density map, distinct axial features repeat every 8 nm (the length of a tubulin dimer; Fig 1A, red rectangle). Most clearly, this is reflected in unequal low-density areas, which can be viewed as holes of different size between intra- and interdimer contacts, and also in various other features of the microtubule map. In addition, the high-density core shows strong axial intradimer contacts and somewhat weaker contacts between dimers. The core of α-tubulin seems slightly lower in density than the core of β-tubulin (for more detail, refer to Krebs *et al*, 2004; Fig 2, upper half). In maps that originate from averaging procedures, such features typically indicate that the subunits adopt different structural flexibilities, and in our case, α-tubulin seems slightly more flexible than β-tubulin. Other differing features can be found on the inside of the microtubule, where loops form large protrusions of a slightly different shape in α- and β-tubulin (Fig 3B, right panel, white arrows).

The interpretation of the recurring differences requires the modelling of atomic data into our map. Initially, the atomic structure of the tubulin dimer from zinc-induced tubulin sheets (1TUB.pdb; Nogales *et al*, 1998) was modelled into our map according to the overall position given by Nogales *et al* (1999). The coordinates were then refined assuming that the tubulin dimer was a rigid body. However, in Zn-sheets, α- and β-tubulin look so much alike that this configuration could not form the structural differences between the subunits that we find in our 17 Å map of an intact microtubule. Unfortunately, the information on microtubules composed of 13 protofilaments (Li *et al*, 2002) does not properly solve that question either. There, the 8 Å structure was calculated using an entirely different approach. In this approach, the subunits along the protofilaments were treated as strings of individual single particles. This approach is outstanding as it opens up the possibility of reconstructing very small particles (the size of tubulin) in an intact microtubule environment. However, we think it is possible that an unintentional merging of different subunits may lead to a structure with identical subunits. In our procedure, although limited in resolution, we took care not to lose the tubulin dimer outline. Consequently, the Zn-sheet configuration had to be adapted to better fit into our map. Therefore, we refined the positions of α- and β-tubulin independently as rigid bodies. This led to the microtubule-tubulin-dimer conformation shown in Fig 1B. In comparison with the Zn-sheet structure, which was used initially, our modelling of the β-subunit showed a small shift in combination with a rotation of $\sim 5^{\circ}$ around a central axis roughly perpendicular to the microtubule lattice plane (Fig 1E). At this position, 3D modelling shows a maximal correlation coefficient of 0.938. Similarly, a maximal correlation coefficient of 0.959 was calculated for the α-subunit after a slight shift and rotation of about 2.8° around a slightly different axis roughly perpendicular to the microtubule lattice plane (these values compare with a value of 0.915 when using the Zn-sheet dimer conformation).

The rotations and shifts lead to upward and downward movements of structural elements responsible for lateral contacts (Fig 1E). Therefore, subunit contacts that have been described earlier (Nogales *et al*, 1999; Li *et al*, 2002) are slightly modified in our microtubule model. Most importantly, our modelling data show shifts of H10, downward shifts of the M-loop and upward shifts of H3 with regard to the positions found in Zn-sheets. These modifications apply to both subunits, but in different magnitudes and with larger movements in the β-subunit. We assume that a downward shift of the M-loop may be related in turn to displacements in other parts of the tubulin molecule, linking our observations to GTP hydrolysis.

The refined tubulin dimer model fits well within the density envelope of the microtubule and tightly modulates the different low-density areas as well as the outer crest (Fig 1C,D). This would not have been possible using the dimer conformation from zinc-induced tubulin sheets without separating the tubulin subunits. The low-density areas of microtubules represent important features, which allow luminal access of small molecules, as has been pointed out previously (Nogales *et al*, 1999; Li *et al*, 2002). In our case, the larger holes (= lower density; Fig 1D) are located at the interface of four adjacent heterodimers, whereas the smaller holes are located in between two neighbouring dimers. The bigger holes are potentially wide enough ($\sim$19 Å) to allow the passage of small molecules, such as taxol, to binding sites on the inside of the microtubule.

Simulations

In general, tracking and identifying individual helices in 3D maps with a resolution lower than 8 Å is impossible. However, maps at poorer resolution can still be used for comparison with simulated maps, which are calculated by reducing the information of atomic data as compared with that of the experimental data. This may indicate whether experimental lower resolution features are

©2005 EUROPEAN MOLECULAR BIOLOGY ORGANIZATION

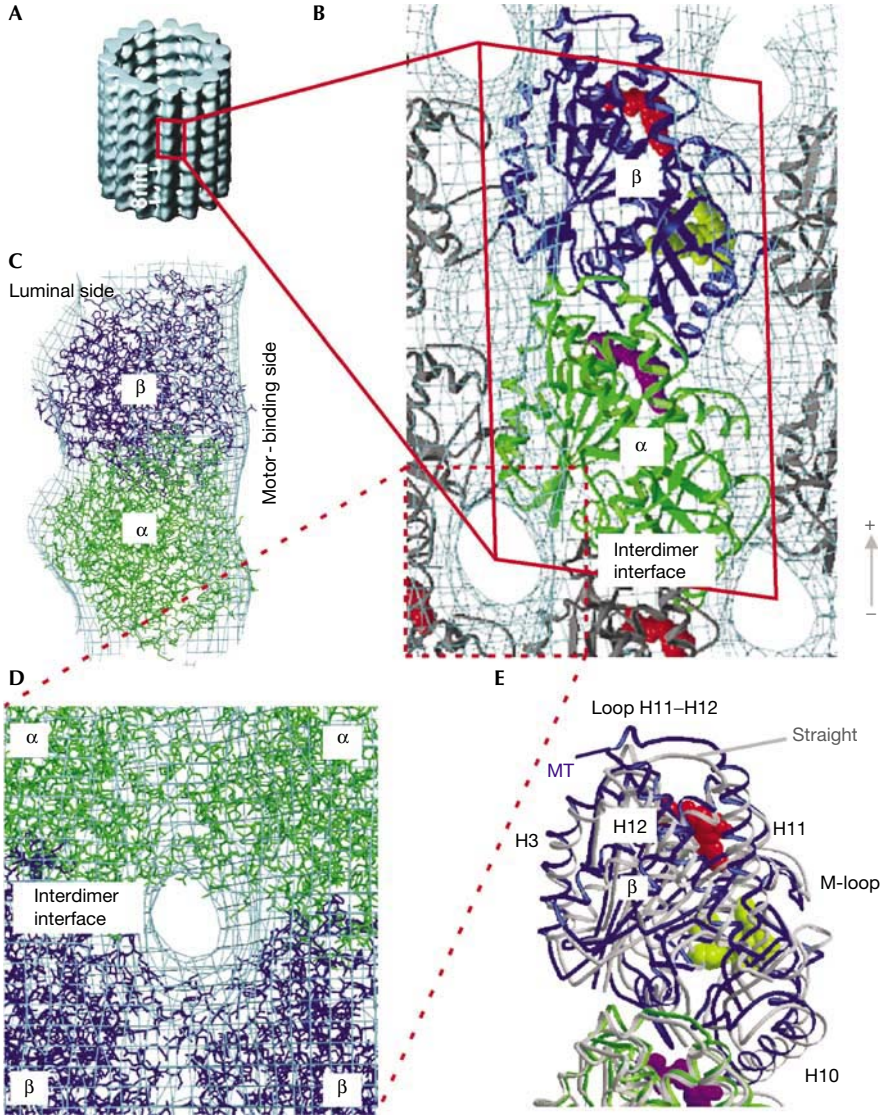

Fig 1 | Structural analysis of the microtubule lattice. (**A**) Surface rendering of the electron density of a 15-protofilament microtubule obtained by cryo-electron microscopy (cryo-EM). Along the microtubule axis, tubulin subunits repeat at ~8 nm. One αβ-tubulin dimer is indicated (red box). (**B**) Fit of the microtubule-tubulin-dimer. Cryo-EM map, light blue; β-tubulin, blue; α-tubulin, green. (**C**) One tubulin dimer in side view. (**D**) Fit of the larger low-density area at the interface of four neighbouring tubulin dimers. (**E**) Enlarged view of β-tubulin to illustrate important structural details as described in the text. GDP, red; GTP, pink; β-tubulin of the microtubule-tubulin-dimer conformation, blue; straight tubulin conformation (Nogales *et al*, 1998), grey; taxol, yellow spheres.

reproducible. If this is the case, conclusions on a molecular scale are still meaningful (Fig 3).

We used the atomic coordinates of our microtubule-tubulin-dimer (Fig 1B) to generate a map reduced in its resolution to 17 Å (Fig 3A), and compared this with our experimental data (Fig 3B). Overall, the strong experimental features are similar, confirming our modelling results. Structural differences between α- and β-tubulin seem slightly more pronounced in the experimental map than in the simulated one. This might be due to the fact that simulations of atomic data to lower resolution lead to an even density distribution that may overemphasize smaller features. However, it is also possible that additional structural differences (in addition to the above-described rotations and shifts) between the underlying atomic coordinates of the tubulin conformation in Zn-sheets and the conformation of tubulin in microtubules may be present.

Straight versus curved conformation

The next question is, how does our model of the microtubule-tubulin-dimer compare with the straight (Zn-sheets; Nogales *et al*, 1998) and curved (tubulin–stathmin complex; Ravelli *et al*, 2004) protofilament conformations, and what are the structural and mechanical connections to microtubule dynamics? We addressed this question by directly comparing all three conformations with

©2005 EUROPEAN MOLECULAR BIOLOGY ORGANIZATION

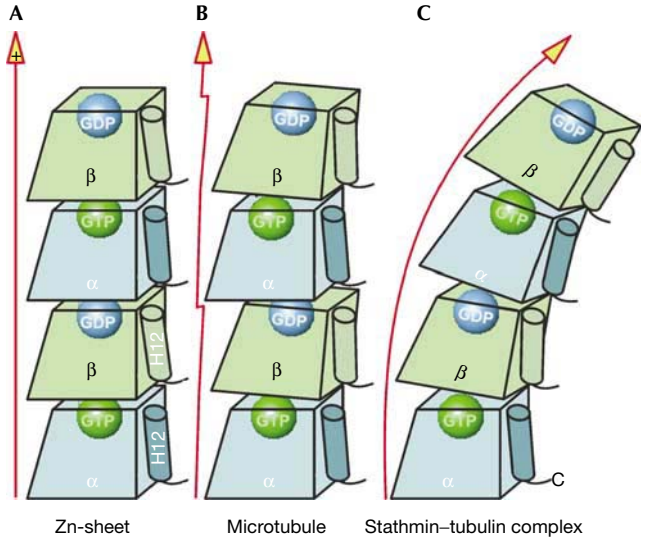

Fig 2 | Schematic diagram showing the mechanism that may trigger rapid depolymerization. (**A**) Straight conformation. (**B**) Microtubule-tubulin-conformation after GTP hydrolysis (this work). (**C**) Curved tubulin conformation. During polymerization, β-tubulin undergoes a structural change following GTP hydrolysis that leads to the indicated 'intermediate' conformation of that subunit (**B**). This conformation is related to the curved conformation and is only stable as long as other tubulin subunits hold the lattice together (in the plus direction of the protofilament). A related conformational change in the α-subunit is much smaller. If the rate of incoming tubulin dimers is too low and GDP-tubulin gets exposed at the plus end of the microtubule, GDP-tubulin may adopt its fully curved (and preferred) conformation (**C**), thereby inducing rapid depolymerization.

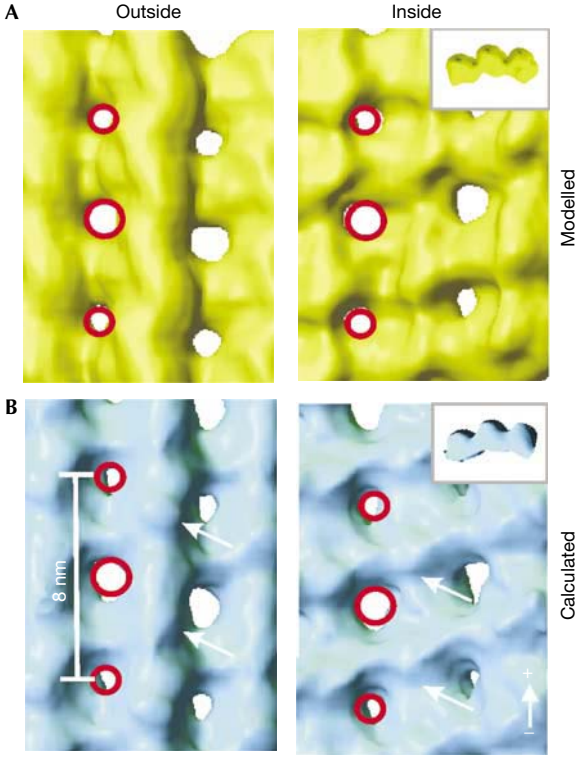

Fig 3 | Comparison of experimental and simulated data. (**A**) Simulation of the microtubule-tubulin-dimer conformation to a resolution comparable with the experimental EM data (~17 Å). Six symmetry-related tubulin dimers (Fig 1B) were used to generate the electron density. The red rings highlight the different sizes of the holes. (**B**) Cryo-electron-microscopy-derived electron density map from microtubules at a similar resolution. The white arrows denote less obvious recurring structural features (at the 8 nm level) that can be seen on the inside and the outside of the microtubule. Electron densities are shown from the outside, the luminal side and in top view (inset).

each other. To better visualize their relationship, we superimposed α-tubulin on each dimer (Fig 4, lower part) and let β-tubulin move according to the different conformations (Fig 4, upper part). We chose α-tubulin for the superposition, because it showed less variability in our modelling attempts. Compared with β-tubulin, the overall fit of α-tubulin was better and the shifts and rotations were smaller.

The three tubulin dimer structures represent the mechanism of the different stages of protofilament bending outwards, away from the microtubule axis. The curvature of the heterodimer increases from straight (Fig 4A, grey), to the structure we find in microtubules (Fig 4A,B, blue), and to the fully curved conformation (Fig 4B, pink). The curved conformation resembles tubulin oligomers after microtubule depolymerization (Mandelkow *et al*, 1991; Muller-Reichert *et al*, 1998). Similarly curved tubulin dimers are also observed in magnesium-induced GDP-tubulin ring structures (Nicholson *et al*, 1999), and in tubulin dimers complexed with Op18/stathmin (Steinmetz *et al*, 2000). The conformational difference between the straight and curved structures was described previously by an overall rotation of the subunits of ~11°, and by a rotation of the second domain relative to the carboxy- and amino-terminal tubulin domains (Ravelli *et al*, 2004). Hence, the tendency to curve outwards seems to trigger depolymerization, similar to the mechanism proposed for KinI (Moores *et al*, 2002).

Structural changes following depolymerization

Our findings have implications on the control of microtubule behaviour (Fig 2). Initially, both tubulin subunits (same nucleotide state) have a similar conformation, which is known to be straight (Fig 2A). Following polymerization, β-tubulin hydrolyses GTP with a slight lag phase, inducing a conformational change in β-tubulin, while transmitting some of the energy into α-tubulin as well. Because of constraints in the microtubule lattice, the tubulin dimer will not be able to adopt a fully curved conformation. Instead, it assumes an intermediate state (Fig 2B), as if trying to curve out completely, but being held back by lateral and axial contacts. In this state, the microtubule may remain intact for some time, but constitutes a less stable state. At the growing end, GTP-β-tubulin subunits adopt the straight conformation and form the GTP cap. This cap seems to be sufficient to prevent microtubule depolymerization, as depolymerization starts from the ends and not from within the microtubule. At low growing rates, GTP hydrolysis catches up with the microtubule plus end and dissolves the GTP-tubulin cap, thereby increasing the chances for depolymerization from that end (see also Caplow *et al*, 1994).

©2005 EUROPEAN MOLECULAR BIOLOGY ORGANIZATION

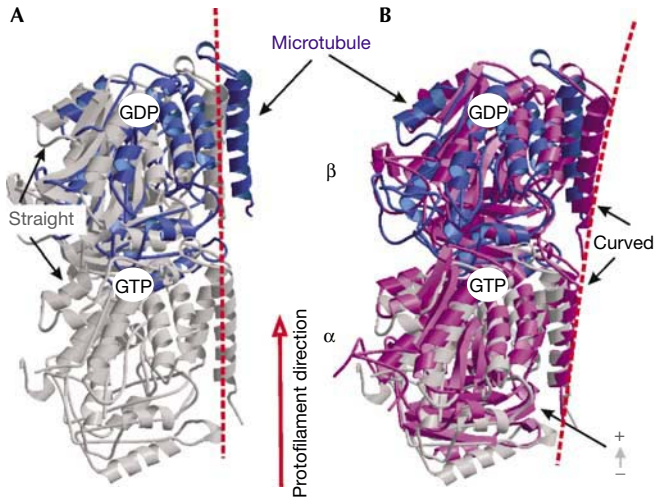

Fig 4 | Relationship of tubulin dimers in intact, helical microtubules (blue) to (**A**) the straight tubulin conformation from Zn-sheets (1TUB.pdb, light grey) and (**B**) to the curved tubulin structure found in the tubulin–stathmin complex (1SA0.pdb, rose). For visualization purposes, the α-subunits are superimposed. One has to remember that the structural differences shown in β-tubulin are the sum of the individual shifts and rotations of both subunits.

The fact that GTP hydrolysis only occurs in β- but not in α-tubulin and the resulting larger conformational changes in β-tubulin may explain the different dynamics at plus and minus ends of microtubules (Mitchison & Kirschner, 1984). At the plus end, β-tubulin is exposed at the outer surface. If growth is slow, GTP hydrolysis occurs on the plus end and changes the conformation of the outermost β-tubulin. This renders the plus end more vulnerable to depolymerization and possibly more accessible to depolymerizing proteins such as KinI (Moores *et al*, 2002). At the minus end, although α-tubulin seems more flexible in our EM map, similarly large modulations are not observed. α-Tubulin contains a non-hydrolysable GTP (the nucleotide is at the N site; Nogales *et al*, 1998), and therefore this end does not change conformation to the same extent as the plus end, rendering the minus end less dynamic.

Native microtubules are very fragile structures, which often depolymerize in seconds. This behaviour strongly impairs cryo-EM work. In addition, for our approach, we need helical microtubules, which are very rare when trying to construct GMPCPP microtubules. For this reason, we are working with taxol-stabilized microtubules. Accordingly, our 3-D reconstruction is that of a stabilized microtubule, and not an entirely plain one. However, we do not believe that this circumstance changes the main message of this paper. We could show that protofilaments in microtubules assume a different structure from those in Zn-sheets. The microtubule structure approaches a somewhat bent configuration, which in turn resembles that of oligomers peeling off a shrinking microtubule. Hence, despite the presence of taxol, our data suggest a plausible model of how microtubules are pre-set for depolymerization.

Concluding remarks

We demonstrated that cryo-EM-derived density maps from helical microtubules composed of 15 protofilaments allow one to distinguish between α- and β-tubulin at 17 Å. We are able to demonstrate that individual structural modifications occur following GTP hydrolysis, suggesting that both subunits have different roles in the microtubule lattice. Rigid-body modelling points towards a conformation of the tubulin dimer within the microtubule lattice that assumes an intermediate state between straight and curved tubulin conformations. We propose a structural model for microtubule depolymerization and show modulations of the microtubule outer surface, which may explain why some cellular components are able to distinguish between GTP- and GDP-tubulin (Severin *et al*, 1997; Schuyler & Pellman, 2001).

METHODS

Modelling and simulation. For this work, an electron density map from helical, taxol-stabilized microtubules composed of 15 protofilaments was used. The electron density map was calculated using a new approach, which is described in detail by Krebs *et al* (2004). In our modelling attempts, the tubulin dimer structure from Zn-sheets (1TUB.pdb; Nogales *et al*, 1998) was fitted into our map in accordance with the overall orientation given by Nogales *et al* (1999). The dimer position was refined as rigid body, and subsequently overall positions of α- and β-tubulin were refined independently using the programme URO (Navaza *et al*, 2002). We directly implemented the helical parameters of a 15-protofilament microtubule in the refinement process. Data from 400 to 17 Å were used in the minimization process. Several optimization cycles were performed until only minimal shifts in the coordinates were observed. To compare our data with the curved tubulin conformation, the atomic data from the tubulin–stathmin complex (1SAO.pdb; Ravelli *et al*, 2004) were also fitted into our map.

Electron density maps were displayed using O (Jones *et al*, 1991) and VOLVIS (Research Foundation of the State University of New York, 1993). Ribbon diagrams were designed using Bobscript (Esnouf, 1997) and Ribbons (Ribbons 3.02 M. Carson, licensed by UAB/CMC). Maps were simulated using CCP4 (The CCP4 suite, 1994).

ACKNOWLEDGEMENTS

We are thankful to J. Borge for help in the usage of the program URO. This work was supported by the Austrian Academy of Sciences (A.K.) and by the 6th Framwework NoE 3D-EM (to A.H.).

REFERENCES

Amos LA (2000) Focusing-in on microtubules. *Curr Opin Struct Biol* **10:** 236–241

Caplow M, Ruhlen RL, Shanks J (1994) The free energy of hydrolysis is stored in the microtubule lattice. *J Cell Biol* **127:** 779–788

Desai A, Mitchison TJ (1997) Microtubule polymerization dynamics. *Annu Rev Cell Dev Biol* **13:** 3350–3359

Downing KH (2000) Structural basis for the interaction of tubulin with proteins and drugs that affect microtubule dynamics. *Annu Rev Cell Dev Biol* **16:** 89–111

Downing KH, Jontes J (1992) Projection map of tubulin in zinc-induced sheets at 4 Å resolution. *J Struct Biol* **109:** 152–159

Esnouf RM (1997) An extensively modified version of MolScript that includes greatly enhanced coloring capabilities. *J Mol Graph Model* **15:** 132–134

Hirokawa N (1994) Microtubule organization and dynamics dependent on microtubule-associated proteins. *Curr Opin Cell Biol* **6:** 74–81

Howard J, Hyman A (2003) Dynamics and mechanics of the microtubule plus end. *Nature* **422:** 753–758

Hyams JS, Lloyd CS (1994) *Microtubules*. New York: Wiley-Liss

©2005 EUROPEAN MOLECULAR BIOLOGY ORGANIZATION

Jones TA, Zou J-Y, Cowan SW, Kjeldgaard M (1991) Improved methods for building protein models in electron density maps and the location of errors in these models. *Acta Crystallogr A* **47:** 110–119

Krebs A, Goldie KN, Hoenger A (2004) Complex formation with kinesin motor domains affects the structure of microtubules. *J Mol Biol* **335:** 139–153

Li H, DeRosier J, Nicholson WV, Nogales E, Downing KH (2002) Microtubule structure at 8 Å resolution. *Structure* **10:** 1317–1328

Ludveña RF (1998) The multiple forms of tubulin: different gene products and covalent modifications. *Int Rev Cytol* **178:** 207–275

Mandelkow E, Mandelkow E-M (1995) Microtubules and microtubule-associated proteins. *Curr Opin Cell Biol* **7:** 72–81

Mandelkow E-M, Mandelkow E, Milligan R (1991) Microtubule dynamics and microtubule caps: a time-resolved cryo-electron microscopy study. *J Cell Biol* **114:** 977–991

Mitchison T, Kirschner M (1984) Dynamic instability of microtubule growth. *Nature* **312:** 237–242

Moores CA, Yu M, Guo J, Beraud C, Sakowicz R, Milligan R (2002) A mechanism for microtubule depolymerization by KinI kinesins. *Mol Cell* **9:** 903–909

Muller-Reichert T, Chretien D, Severin F, Hyman AA (1998) Structural changes at microtubule ends accompanying GTP hydrolysis: information from a slowly hydrolysable analogue of GTP, guanylyl (α, β)-methylenediphosphonate. *Proc Natl Acad Sci USA* **95:** 3661–3666

Navaza J, Lepault J, Rey FA, Alvarez-Rua C, Borge J (2002) On the fitting of model electron densities into EM reconstructions: a reciprocal-space formulation. *Acta Crystallogr D* **58:** 1820–1825

Nicholson WV, Lee M, Downing KH, Nogales E (1999) Cryo-electron microscopy of GDP–tubulin rings. *Cell Biochem Biophys* **31:** 175–183

Nogales E (2001) Structural insight into microtubule function. *Annu Rev Biophys Biomol Struct* **30:** 397–420

Nogales E, Wolf SG, Downing KH (1998) Structure of the alpha beta tubulin dimer by electron crystallography. *Nature* **391:** 199–203

Nogales E, Whittaker M, Milligan RA, Downing KH (1999) High-resolution model of the microtubule. *Cell* **96:** 79–88

Ravelli RBG, Gigant B, Curmi PA, Jourdain I, Lachkar S, Sobel A, Knossow M (2004) Insight into tubulin regulation from a complex with colchicines and a stathmin-like domain. *Nature* **428:** 198–202

Schuyler SC, Pellman D (2001) Microtubule 'Plus-end-tracking proteins': the end is just beginning. *Cell* **105:** 421–424

Severin FF, Sorger PK, Hyman AA (1997) Kinetochores distinguish GTP from GDP forms of the microtubule lattice. *Nature* **388:** 888–891

Steinmetz MO, Kammerer RA, Jahnke W, Goldie KN, Lustig A, van Oostrum J (2000) Op18/stathmin caps a kinked protofilament-like tubulin tetramer. *EMBO J* **19:** 572–580

The CCP4 Suite (1994) Programs for protein crystallography. *Acta Crystallogr D* **50:** 760–763

©2005 EUROPEAN MOLECULAR BIOLOGY ORGANIZATION